Severe Convective Windstorms over the Northern High Plains of the United States

BRIAN A. KLIMOWSKI AND MATTHEW J. BUNKERS

National Weather Service, Rapid City, South Dakota

MARK R. HJELMFELT AND JOSIAH N. COVERT*

South Dakota School of Mines and Technology, Rapid City, South Dakota

ABSTRACT

During the warm seasons (May–September) of 1996–99, Weather Surveillance Radar-1988 Doppler (WSR-88D) data and severe wind reports (either gusts >25 m s^{-1}, or damage-related reports) over the northern High Plains (NHP) of the United States were analyzed in order to document the primary modes of convection responsible for severe winds. It was found that two-thirds of the convectively generated severe wind reports over the NHP were identified as being produced by organized convective structures rather than by isolated downburst or microburst activity. Specifically, at least 29% of all severe wind reports were produced by bow echoes, 20% by squall lines, 9% by supercell thunderstorms, and 7% by other convective systems not organized in a linear fashion. The occurrence of linear convective storm types that typically produce high winds (i.e., squall lines and bow echoes) were also documented over the NHP during the period of study. It was found that 51% of all squall lines and 86% of all bow echoes were associated with severe surface winds. There was a preference for these storms to initiate near the interface of the Rocky Mountains and the plains [~66% formed within 120 km (75 miles) of significant topography], and their typical lifetime was 2–4 h. Also of interest, bow echoes had 3 times the number of severe wind reports as severe hail reports, while this ratio was 1.6 for squall lines, and only 0.6 for supercells. The results from these analyses indicate that the nature and evolution of squall lines and bow echoes over the NHP illustrate some differences from similar storms over other regions. Trailing areas of stratiform precipitation were observed to be less common with squall lines over the NHP than other areas. Back-building squall lines were observed less frequently over the NHP, when compared with the southern plains. It was found that storm mergers were associated with the initiation of 41% of the bow echoes and that significant severe wind events occasionally occurred without any linear organization.

1. Introduction

According to the results of Kelly et al. (1985, p. 1999), severe thunderstorm winds (either gusts >25 m s^{-1}, or damage-related reports) account for approximately 61% of the total number of severe thunderstorm reports (i.e., hail and wind) across the United States. Although a few studies provide insight into the convective modes associated with severe winds at the surface (e.g., Bluestein and Jain 1985; Johns and Hirt 1987; Atkins and Wakimoto 1991), comparatively little is known about the relative frequency of parent convective systems that produce these severe and damaging winds. With the sparse population and observation network over the northern High Plains (NHP)—herein defined as the area west of the central Dakotas and central Ne-

braska, and east of the Rocky Mountains (Fig. 1)—even less is known about the relative significance, frequency, and mode of severe convective windstorms over this area.

Existing research on severe-wind-producing convective systems covers a wide variety of convective storm types, including small microburst-producing storms (e.g., Fujita 1981; Wakimoto 1985), high-precipitation (HP) supercells (Moller et al. 1994), bow echoes (e.g., Przybylinski 1995; Weisman 2001), squall lines (e.g., Bluestein and Jain 1985; Smull and Houze 1985), and mesoscale convective systems and complexes (MCSs and MCCs: Maddox 1980; Schmidt and Cotton 1989). These convective modes cover a substantial range of time- and space scales, spanning from less than an hour and a few kilometers on the lower end to several hours and several hundreds of kilometers on the higher end of the spectrum. Advances in our understanding of these topics have been made over the past decade or two (e.g., Weisman 2001; Wakimoto 2002), especially with respect to the storm dynamics controlling the formation and evolution of these systems (e.g., Rotunno et al.

---

* Deceased.

Corresponding author address: Dr. Brian A. Klimowski, National Weather Service, 300 East Signal Dr., Rapid City, SD 57701-3800.
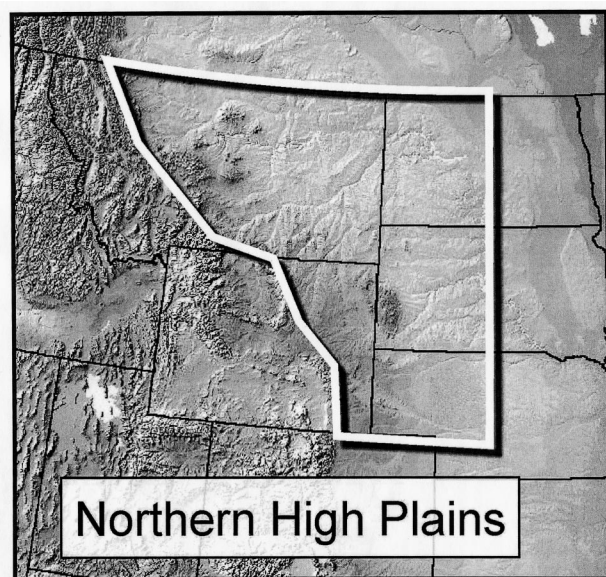E-mail: brian.klimowski@noaa.gov

Fig. 1. The NHP area as defined in this article (outlined in white).

1988; Weisman 1992, 1993), as well as the atmospheric environments in which these storms form (e.g., Johns and Hirt 1987; Evans and Doswell 2001).

Kelly et al. (1985) speculated that a large percentage of the convectively produced severe winds over or near the NHP was a result of weaker thunderstorms associated with isolated, microburst events. Since their research was published, the national network of Weather Surveillance Radar-1988 Doppler (WSR-88D) radars has made the investigation of this hypothesis feasible. Accordingly, observations by operational forecasters in the NHP have suggested that *organized* convection might actually be responsible for the majority of these high wind events, as opposed to isolated microburst-producing systems. In light of this, a research project was initiated in 1996 to investigate severe wind-producing convective events, as well as linear convective systems, over the NHP.

The primary goal of the present research is to increase the ability of forecasters to anticipate the production of severe winds from convective storms over the NHP. Specifically, this includes the following objectives: (i) to identify the types of convective events responsible for the production of severe surface winds, (ii) to gain a greater understanding of the evolution and structure of these high-wind-producing systems, (iii) to gain a greater understanding of the evolution and structure of *linear* convective systems (squall lines and bow echoes), (iv) to identify the characteristic environments in which these systems form, and (v) to determine if the lifetimes and convective modes of severe convective windstorms across the NHP are similar to those in other parts of the country. Last, in order to develop a reference frame from which to better understand our results, a detailed climatology of high wind reports and severe weather pa-

rameters related to severe convective storms is produced. Therefore, in this paper, we provide an analysis of the evolutionary characteristics and atmospheric environments of organized, severe, nontornadic, convective windstorms over the NHP.

2. Nature of the dataset and description of the analyses

a. Overview and general methodology

The NHP as defined in this study includes the elevated, mostly treeless U.S. plains west of the Missouri River and east of the Rocky Mountains, generally north of 41°N and west of −100°W (Fig. 1). The NHP region generally slopes down from elevations well above 4000 ft (1220 m) MSL on the western periphery, to less than 2000 ft (600 m) MSL on the eastern edge of the area. Most of the NHP falls within the "western plains region" as defined by Easterling and Robinson (1985), which is characterized by a strong diurnal signal in the frequency of convection, as well as a broad transition zone in the time of maximum convective frequency (e.g., Court and Griffiths 1986). These analyses suggest a preference for storms to initiate near the Rocky Mountains late in the afternoon, and to mature as they move east during the evening. For example, along the western edge of the NHP (eastern terminus of the Rocky Mountains), the preferred time of maximum convective activity is around 1600–1700 LST; and along the eastern edge of the NHP (central Dakotas), the time of maximum convective frequency is 2200–2400 LST. A climatology of MCCs from 1977 to 1983 shows a similar evolutionary pattern, with the NHP representing an "initiation zone" for MCC development (e.g., McAnelly and Cotton 1989, their Fig. 1).

An effort was made to document all severe wind-producing convective systems from 1996 through 1999 over the NHP, as well as all squall lines and bow echoes (the various convective modes will be formally defined in the next paragraph). This was accomplished through the daily perusal of the radar data across the region, and the analysis and investigation of severe wind reports throughout the convective season. If two or more severe wind reports were noted in a pattern that suggested that they might have originated from the same storm, radar data were acquired to investigate the type of storm responsible for the production of these severe winds. From the collection of data in this way it was anticipated that the majority of severe-wind-producing convective systems over the NHP from 1996 through 1999 (as well as those systems that are typically associated with severe winds—bow echoes and squall lines) could be quantitatively analyzed over the NHP.

b. The storm dataset and definitions

The primary convective storm types (squall lines, bow echoes, and supercell thunderstorms) were deter-

mined using definitions consistent with those in the recent and historical literature. Our criteria to identify squall lines were roughly the same as Bluestein and Jain (1985) and the OFCM (1980). Squall lines were required to have a radar reflectivity length-to-width ratio of at least 5:1, exhibit convective cells along a line at least 50 km long, and persist for greater than 30 min. A squall line as defined above could have been composed of (or evolved into) other organized convective structures, such as supercells and bow echoes. Note that this definition includes much smaller events (in space and time) than the ''linear MCS'' definition of Parker and Johnson (2000). The criteria we used to identify bow echoes were consistent with the definitions of Fujita (1978) and Klimowski et al. (2000). A bow echo was defined as a bow or crescent-shaped radar echo with a tight reflectivity gradient on the convex (leading) edge, the evolution and horizontal structure of which were consistent with storms that propagate along a strong outflow. Thus, the bowing echo was required to exhibit an increasing radius with time or a persistent arc, which demonstrates linear organization, rather than a coincident (brief) grouping of cells into an otherwise unassociated arclike structure. Our definition includes the full range of bow echoes, whether isolated (singular), or embedded within a larger-scale convective system (such as a squall line). Radar features such as rear-inflow notches or strong rear-inflow jets might give insight into the severity of the bow echo, but were not required for it to be defined as such. High-wind-producing supercell thunderstorms were defined in accordance with Moller et al. (1994), and were required to have at least two severe wind reports. Reflectivity data were adequate in most cases to identify discrete supercells—with the characteristically distinctive reflectivity features and deviant motion. If there was a question of the rotation of the storm, the velocity data were consulted (less than 10% of the supercells required the use of velocity data). If a storm was associated with three or more severe wind reports and did not demonstrate linear organization, and was not a supercell, it was placed in a category we refer to as ''irregular'' (the greater number of severe winds for this category, relative to the others, was needed to separate it from groupings of two otherwise isolated events).

c. Organization and partitioning of the storm dataset

MCSs and MCCs frequently exhibit very complex radar reflectivity patterns and evolutions. The high wind events identified over the NHP occasionally occurred as a part of the evolution of a large MCS or MCC. It was not uncommon for one severe-wind-producing convective mode to evolve into another (as seen in the radar imagery). There were 39 occurrences of such an evolution in the NHP data, all of which were either squall-line–bow echo or supercell–bow echo transitions. The occurrence of one high-wind-producing morphology

within another, however, was quite rare in the NHP dataset (there were only four cases where bow echoes occurred within larger-scale squall lines, and two cases where high-wind-producing supercells occurred within squall lines).

When one type of severe-wind-producing event evolved into (or occurred within) another, each discrete high-wind-producing storm was treated (counted) separately, each with their own points of initiation and dissipation, and each with a uniquely calculated duration. The time and position of any severe weather reports at the surface were carefully noted in order that they could be correctly associated with the appropriate storm. Using this type of partitioning, there was no overlap in the grouping of these severe-wind-producing convective storms (each event was partitioned in time and space into its respective high-wind-producing convective components). In this way, 143 convective severe-wind-producing storms (components) were identified over the NHP from 1996 through 1999 (28 supercells, 56 bow echoes, 47 squall lines, and 12 irregular groups). In addition, 46 nonsevere squall lines, and nine nonsevere bow echoes were analyzed. Seventeen events exhibited more than three related high wind reports but did not have sufficient radar data to identify their structure (hereinafter referred to as ''unknown''). The balance of the severe wind reports not associated with the aforementioned events were isolated in nature, and not assumed to be a part of any organized high-wind-producing system.

d. Radar data acquisition and analysis

In order to make an accurate determination of the attributes, duration, and evolution of the various convective morphologies, WSR-88D data (5- to 15-min resolution) were utilized for these analyses. WSR-88D reflectivity and velocity data archives from individual radar sites, as well as WSR-88D 0.5° reflectivity mosaic data (2-km resolution across the United States), were used for this purpose. For each case, the focus of the analyses was on the evolutionary history of the system and its relation to severe weather. The time and location of the initiation and dissipation of each discrete convective mode (as defined in section 2b), and transitions between modes, were documented. In addition, all reports of severe weather during the events were scrutinized to identify the relationship between the severe weather and the particular convective mode.

As was noted previously, the NHP is a sparsely populated region with few trees or crops, and severe winds will frequently not be reported or cause any significant damage. This undersampling will impact the results of these analyses in several ways, but in general we have to assume that there was more severe wind than was reported, and that several of the ''isolated'' reports were probably associated with unreported significant events. It is assumed that while not an exhaustive compilation,

these analyses should represent the great majority of high-wind-producing systems over the NHP.

e. National Weather Service radiosonde observations

For each high wind or linear convective event, we attempted to characterize the preconvective environment (in which the storm initiated and evolved) through the use of unmodified, uninterpolated, radiosonde observations. Each sounding was investigated for continuity with the large-scale environment and checked for erroneous and unrepresentative data (e.g., bad surface data, incomplete flights, convective contamination, etc.). In order to ensure the appropriateness of the soundings to a particular event, the radiosonde data were also required to be within 250 km and 3 h of the formation of the convective mode in question. Applying a threshold to the data in this way limited the radiosonde environmental analyses to 104 (of a possible 198) cases, of which 48 were associated with squall lines, 28 with bow echoes, 19 with supercells, and 9 with irregular groups. Nine of the soundings characterized the environments of more than one convective mode. This occurred when the evolution from one high-wind-producing morphology into another occurred close to the location and time of the sounding, or when different severe-wind-producing storm types occurred near the sounding location, but at some distance from each other.

3. Climatology of convectively generated severe winds over the NHP

a. Severe wind and hail climatologies

In order to develop a reference frame for our research, climatologies of the severe convective winds across the NHP (and other areas) were produced. All severe wind and hail reports from 1955 through 1995 were extracted from the historical severe weather archives produced at the Storm Prediction Center (SPC). The SeverePlot software (Hart and Janish 1999) was used to analyze these data. It was found that 40% of the severe weather reports over the NHP were from wind [as compared with 61% nationally, as reported in Kelly et al. (1985)].

Two different analyses were performed with the SPC historical severe weather archives to determine the characteristics of convective severe wind reports over the NHP. These included a spatial analysis, which highlighted geographical regions with higher frequencies of severe wind reports, and a temporal analysis, which focused on the frequency of severe wind reports as a function of the time of day.

1) Spatial analysis

The spatial distribution of all the severe convective wind reports from 1955 through 1995 encompassing the NHP shows some interesting features (Fig. 2). There
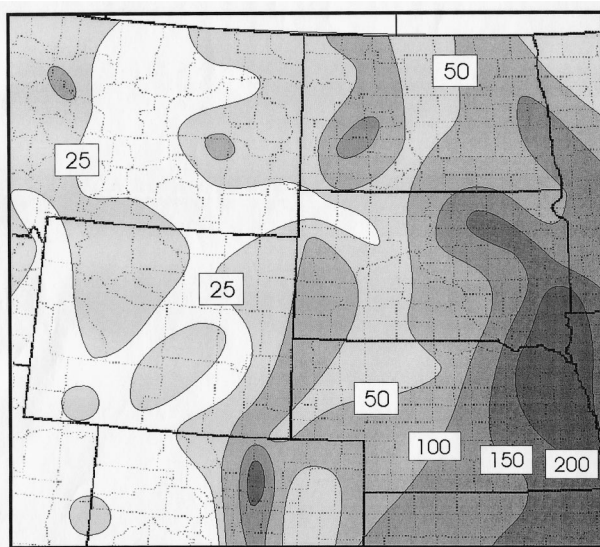
Fig. 2. Spatial distribution of convectively generated severe wind reports across the NHP and surrounding area from 1955 through 1995. Data are analyzed and shaded every 50 reports per 10 000 km^2.

are three primary maxima in the severe wind frequency: (i) one located in western North Dakota, (ii) one extending from the Black Hills southward along the Front Range of Wyoming and Colorado, and (iii) a larger maximum extending to the southeast from the central Dakotas. The climatological analysis in Fig. 2 largely represents the northwestern edge of a frequency maximum, which extends well to the southeast into the central plains and the mid-Mississippi River valley.[1]

While there is no doubt that this distribution is heavily influenced by population density (e.g., see discussion by Johns and Evans 2000), there are other factors that may be influencing the observed pattern. First, the preference for convection to initiate and occur over the elevated terrain near the western High Plains (e.g., Zajac and Rutledge 2001), combined with the relatively dry atmosphere, can account for the maximum located in western South Dakota, and along the Front Range of Colorado, Wyoming, and Montana. Second, the fact that thunderstorms are more common southeast of the NHP (Changnon 2001; Orville and Huffines 2001) could partially explain the maximum of severe wind reports in this area.

Another partial explanation for the greater number of high wind reports in the eastern part of the NHP (Fig. 2) is that there are considerably more trees east of the Missouri River, which lend themselves to more damage-based reports for winds (broken tree limbs and fallen trees count as evidence of severe winds for severe weather verification). Indeed, a review of the SPC his-

---

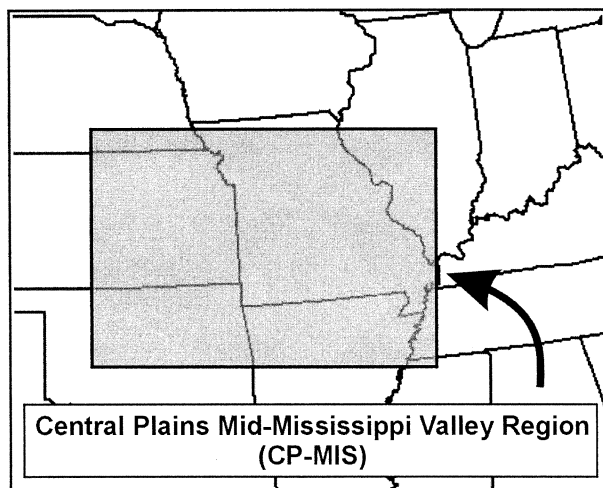[1] For a more thorough spatial analysis of the severe thunderstorm winds across the United States, see information online at http://www.nssl.noaa.gov/hazard/ and Doswell and Bosart (2002).

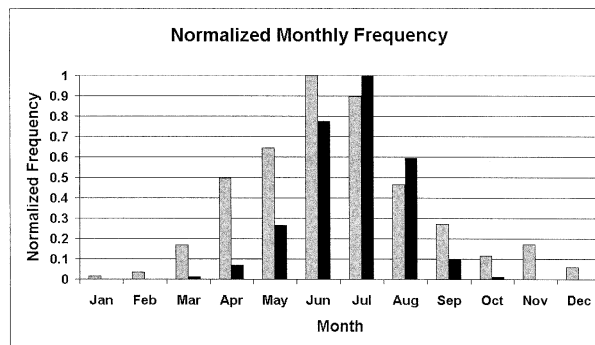FIG. 3. The CP-MIS region as defined in this article.

FIG. 4. Histogram of the normalized monthly distribution of convectively generated severe wind reports over the NHP (black) and the CP-MIS (gray). Data are normalized to the greatest monthly value.

torical severe weather archives from 1955 to 1995 shows that an average of 43% of the severe wind reports are damage-based across the contiguous United States, as compared with only 10% over the NHP. In areas where trees grow extensively (such as the northeastern United States), nearly 70% of the severe wind reports are damage based. It is clear that with the current method of verifying and identifying severe winds nationally, the distribution of trees will have a great impact on the appearance of any spatial severe wind distribution that uses these data. With the lack of population and trees over the NHP, it is difficult to get a reliable estimate of the spatial severe wind distribution. It is anticipated that using radar data to identify and track the storms responsible for the production of severe winds will help us to clarify the nature of this distribution.

2) TEMPORAL ANALYSIS

The seasonal and diurnal variations of severe wind observations were also calculated over the NHP. In order to compare these variations with those over a climatologically different area where much study has been performed on convective windstorms, an analysis of the seasonal and diurnal variations of severe wind observations over the central plains mid-Mississippi valley region (CP-MIS: herein identified as a similarly sized area centered over southwestern Missouri) was also performed (Fig. 3).

Analysis of the seasonal distribution of severe winds demonstrate that the majority of severe winds over the NHP occur during the summer months of June, July, and August (Fig. 4). Eighty-six percent of the severe winds occur during these months, with July being the month of the greatest frequency of severe winds. The frequency of severe winds over the CP-MIS is about three times that in the NHP, with June being the month of the greatest number of severe wind reports. The dis-

tribution of severe winds is also spread over a longer period in the CP-MIS, with five months composing >40% of the peak monthly value. One characteristic that distinguishes the NHP from the CP-MIS is the strong diurnal dependence of the frequency of high wind reports (Fig. 5). For example, during the 3-h period of greatest high wind frequency across the NHP [1800–2100 central daylight time (CDT)], 1379 high wind reports were recorded from 1955 to 1995. This is over 90 times the amount that occurred during the 3-h period from 0800–1100 CDT, during which only a total of 15 severe wind reports were recorded. By way of comparison, temporal analyses performed over the CP-MIS exhibited around seven times the difference between the maximum and minimum frequency periods. Furthermore, similar analyses performed over the entire United States revealed only about 8 times the difference between the most and least active 3-h periods of convective high wind reports (Kelly et al. 1985). These results complement the general observations of Easterling and Robinson (1985), namely, severe wind gusts associated with thunderstorms across the NHP (and the High Plains in general) have a very strong diurnal dependence (similar to the general diurnal trends of thunderstorms in this area).

b. Regional convective parameter climatologies

Previous convective windstorm research (e.g., Fujita 1978; Bluestein and Jain 1985; Przybylinski 1995; Bent-
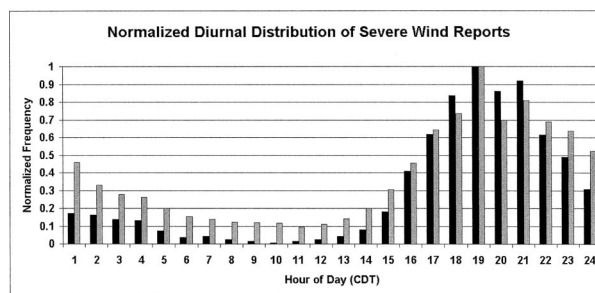

FIG. 5. Same as in Fig. 4 but for the hourly distributions.

ley and Mote 1998; Evans and Doswell 2001; to name a few) has generally focused on areas outside the NHP. In an effort to compare the convective environments of the NHP with a climatologically different area (the CP-MIS), a climatological analysis of several sounding parameters (i.e., buoyancy, moisture, and shear) relevant to convective windstorms was performed. This analysis may help to explain, or to suggest, differences in the nature and evolution of severe convective wind events between the above-mentioned regions.

Radiosonde data from 1948 to 2000 were gathered for four sounding sites in the NHP (Rapid City, South Dakota; Bismarck, North Dakota; Glasgow, Montana; Great Falls, Montana), and for four sites in the CP-MIS (Lincoln, Illinois; Springfield, Missouri; Topeka, Kansas; Norman, Oklahoma). To best represent the convective seasons of both the NHP and the CP-MIS, all soundings from March through October were investigated. The sounding data were obtained either from the National Climatic Data Center (NCDC) radiosonde database archive available on CD-ROM for 1948–97, or from the Forecast Systems Laboratory (FSL) online radiosonde database archive for post-1997 data (raob.fsl.noaa.gov). It is noted that some of the eight sounding sites represent composites from two or three sites [e.g., Norman contains data for Norman (OUN), Tinker Air Force Base (TIK), and Oklahoma City (OKC) because of several station moves]. More information on the radiosonde quality control and parameter calculations can be found in the appendix. The composited data are not expected to be a problem since a general climatology of the two respective regions was desired, and all sounding data were subsequently combined for each of the two regions. The *median* values of the sounding parameters were used (rather than the *mean* values) to demonstrate the strongest signals of this highly variable, and very large, dataset (Fig. 6) so that erroneous outliers would not influence the values significantly. The size of this dataset (20 000–30 000 soundings) required that automated data quality checks be employed, but these could not remove all erroneous outliers.

The surface-based parcel was used to calculate relevant convective parameters in lieu of other available choices, because it is believed that most convective high wind events result from surface-based convection (as opposed to elevated convection). Only those soundings that possessed both a SBCAPE >50 J kg^{-1} and a SBCIN <50 J kg^{-1} were utilized, which means that all other parameters are conditional on these two constraints. These thresholds were chosen as indicative of environments capable of producing deep moist convection, independent of the time of day. Early morning soundings (1200 UTC) accounted for less than 10% of those used in these analyses but were included in these analyses to represent that small fraction of convective events that occur around this time. Even though the soundings used in these analyses were unmodified, the constraints out-lined above should ensure that the general features of the convective environments were adequately characterized.

The climatological analysis of the sounding parameters from 1948 to 2000 supports the notion that the peak in the severe weather season across the NHP is from June to August, and across the CP-MIS it is primarily in the spring to early summer. This represents the time when the CAPE is strongest in the NHP, and when vertical wind shear—in the presence of instability—is generally the strongest in the CP-MIS (Fig. 6). The more significant findings from the sounding climatology are as follows:

- Median positive SBCAPE values (Fig. 6a) consistently range from 250 to 1000 J kg^{-1} lower across the NHP when compared with the CP-MIS, but the median SBCIN (Fig. 6e) is also less (closer to zero) in the NHP.
- The median 0–1-km mixing ratios (Fig. 6d) are significantly lower across the NHP when compared with the CP-MIS. Note that the median NHP values are consistently below the 10th percentile of the CP-MIS values. This mirrors the difference in precipitable water values (not shown), the medians of which are 0.40–0.70 in. lower across the NHP.
- Median SBLCL heights (Fig. 6c) are consistently higher across the NHP when compared with the CP-MIS.
- Median total 0–3-km vertical wind shear (Fig. 6b) is fairly constant over the NHP. There is a weak signal in the data that shows that the 0–3-km total shear may follow an annual cycle over both regions with minimum values in the CP-MIS during mid- to late summer, even as maximum values are occurring in the NHP.
- There is little significant seasonal change in the median bulk 0–3-km vertical wind shear (Fig. 6f) over the NHP and the CP-MIS. However, these data suggest a slight inverse relationship between the NHP and CP-MIS, with a peak in July over the NHP and a minimum in the mid- to late summer across the CP-MIS.

The differences in Fig. 6 are likely the result of diminished low-level moisture across the NHP (as would be expected for this semiarid region), as well as the annual cycle in vertical wind shear across the CP-MIS (i.e., the northward progression of the jet stream and the increase of southeast flow over the NHP during the summer). Less available low-level moisture in the NHP leads to less CAPE [and hence a smaller bulk Richardson number (BRN); Fig. 6h] and higher cloud bases. The higher cloud bases in the NHP result in a deeper subcloud layer for evaporative acceleration of downdrafts, but this may also act to shorten the life span of convection because of the outflow outrunning its parent thunderstorm.
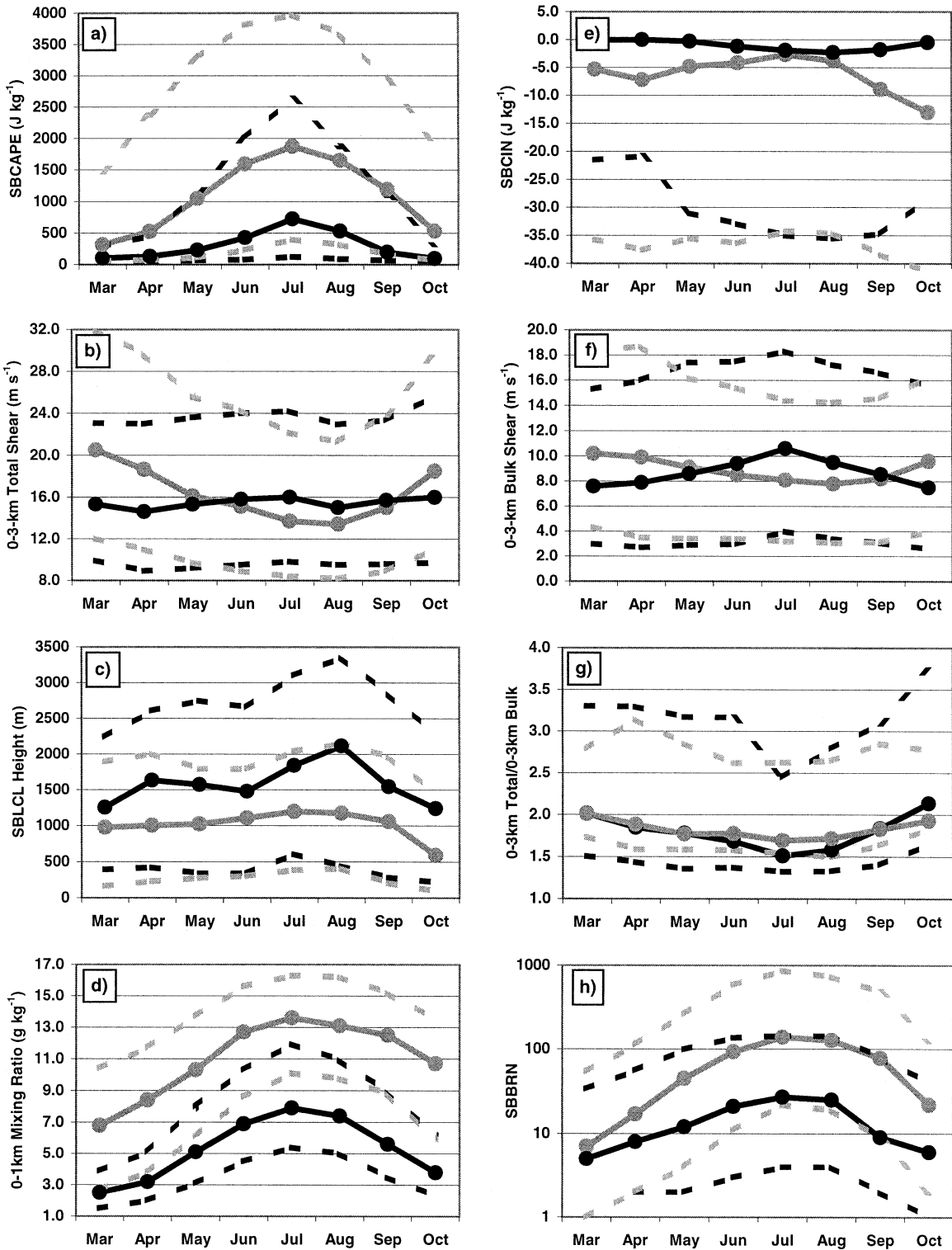
FIG. 6. Median (solid lines) and 10th/90th percentile (dashed lines) values of convective parameters derived from the analysis of radiosonde data over the NHP (black) and the CP-MIS (gray). Monthly values are given over the primary convective seasons (Mar–Oct). The convective parameters include (a) surface-based convective available potential energy (SBCAPE), (b) 0–3-km total shear, (c) surface-based lifting condensation level (SBLCL), (d) 0–1-km mixing ratio, (e) surface-based convective inhibition (SBCIN), (f) 0–3-km bulk shear, (g) 0–3-km total shear/0–3-km bulk shear, and (h) surface-based bulk Richardson number (SBBRN).

TABLE 1. Summary of the convective events observed over the NHP from 1996 through 1999.

	Total events	Severe wind events	Severe wind reports (% of total)	Reports per severe event	Reports per hour	Ratio of severe wind/hail	Life span (h)
Squall lines	93	47	170 (20%)	3.6	0.9	1.6	3.2, 3.8 severe, 2.6 nonsevere
Bow echoes	65	56	243 (29%)	4.3	1.3	2.9	3.2, 3.4 severe, 1.8 nonsevere
Supercells		28	79 (9%)	2.8	0.7	.59	3.9
Irregular		12	60 (7%)	5.0		5.0	
Unknown		17	54 (6%)	2.9			
Isolated			248 (29%)				

4. Observed structure of severe wind events

a. Overview of the NHP analyses

As described earlier, the observed high-wind-producing storms over the NHP were partitioned into the four categories: (i) squall lines, (ii) bow echoes, (iii) supercells, and (iv) irregular groups. If radar data were not available for a particular event, and it was associated with three or more severe wind reports, it was placed in the ''unknown'' category. This category includes those systems that appear to have high-wind-producing storm-scale organization, but the radar data were inadequate to identify the specific storm type.

From 1996 through 1999, 854 high wind reports were recorded over the NHP (Table 1). Of these, 552 (65%) reports were associated with 143 separate organized high wind events for which radar data were acquired for analysis (an average of 3.9 reports per event). (Radar data were collected for an additional 46 squall line and nine bow echo cases in which severe winds were not observed.) There were 17 high wind events with at least three severe wind reports in which adequate radar data were not available (the unknown category); these accounted for 54 of the severe wind reports (6% of the total). The remaining 248 high wind reports (29% of the total) were categorized as isolated wind reports, most likely associated with microbursts, or some other disorganized or short-lived convection. These data also indicate that at least 64% of the organized high wind events over the NHP were squall lines or bow echoes (Table 1). These two linear storm types accounted for 75% of the severe wind reports associated with the four categories listed above, or 49% of the total severe wind reports reported across the NHP. Only four of these events met the criteria of a derecho as defined by Johns and Hirt (1987).

The life span[2] of the severe wind events analyzed over the NHP was between 3 and 4 h (Table 1). Squall lines and bow echoes associated with severe winds tended to be longer lived (3.8 and 3.4 h, respectively) than those that were nonsevere (2.6 and 1.8 h). High-wind-

producing supercells, on average, persisted the longest (3.9 h). It is interesting to compare the duration of these events with the life spans observed in several comprehensive analyses of MCSs in the literature. In a study over the central United States, Parker and Johnson (2000) found that linear MCSs had a mean life span of 10.5 h; systems possessing trailing stratiform regions lasted nearly twice as long as those with leading or along-line stratiform areas (12.2 versus 6.4 h, respectively). Geerts (1998) analyzed a number of MCSs over the southeastern United States and found their mean life span to be around 9 h. Though the broader definitions of life span (and MCS) would naturally tend to increase the observed duration of these events, it appears that there may be some evidence suggesting the severe-wind-producing convective systems over the NHP are (on average) shorter lived than similar storms that form to the south and east of the NHP.

The distribution and extent of the convective events analyzed in this study can be seen in Fig. 7, which illustrates the tracks of the observed squall lines, bow echoes, and severe-wind-producing supercells in this study. Additionally, the points of initiation for all these events (Fig. 7d) are shown relative to the approximate location of the interface between the Rocky Mountains and the NHP. It is apparent from Fig. 7 that the distribution of squall lines and bow echoes that occur within the NHP is fairly uniform across the area. There appear to be enhanced concentrations of events north of the Black Hills of South Dakota, extending from northwestern South Dakota through south-central North Dakota. In general, the majority of squall lines and bow echoes moved eastward or northeastward, and occurred generally during the same time of day (the diurnal frequency of the events mirrored the tendency of the observed high wind reports in Fig. 5).

b. Squall lines

Ninety-three squall lines were observed over the NHP from 1996 to 1999, 47 of which (51%) were associated with severe winds (Table 1). Squall lines accounted for 29% of the organized high wind events identified, and were responsible for producing at least 20% of the total number of severe wind reports. Severe winds occurred 1.6 times more frequently than severe hail in the ob-

---

[2] Herein, life span is defined as that period of time in which the criteria for identifying a particular mode of convection were met, regardless of where it dissipated. Note that this definition is more specific than that of the MCS definitions in Geerts (1998) and Parker and Johnson (2000).
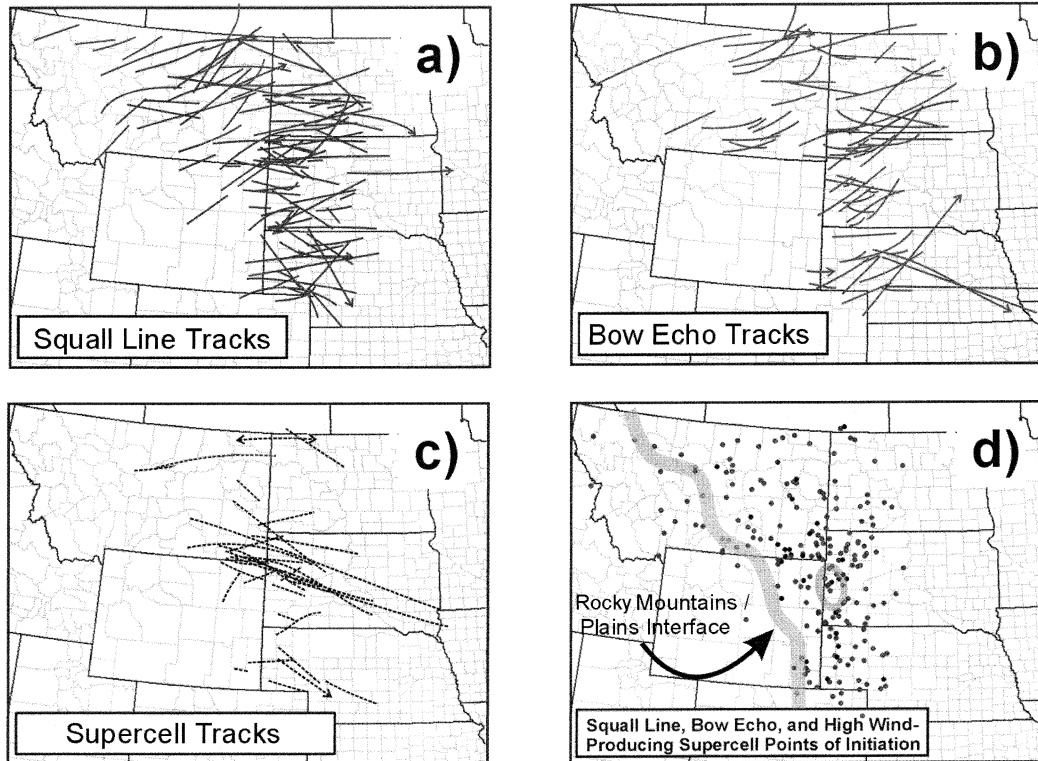
Fig. 7. Tracks of the high-wind-producing convective events over the NHP from 1996 through 1999 for (a) the observed squall lines, (b) the observed bow echoes, and (c) the observed severe-wind-producing supercells. (d) Points of initiation for the squall lines, bow echoes, and supercells. Arrows on either end of a storm track indicate that the corresponding begin/end time is not known because of a lack of radar data.

served squall lines. A slight preference for severe hail to occur early in the life of the squall lines was also evident, but there was not a significant association between severe wind occurrence and the maturity of the system. Squall lines were generally a ''terminal'' convective morphology; that is, in the majority of cases, the squall line was the last organized structure prior to dissipation. In 13% of the cases, the squall line acted

as an ''intermediate'' structure—with the squall line later evolving into a bow echo.[3] Representative examples of severe squall lines observed over the NHP are shown in Fig. 8. On four occasions, squall lines were observed

_____

[3] A squall line that evolved into a bow echo was counted separately from the bow if the squall line met the squall-line definition in section 2a.
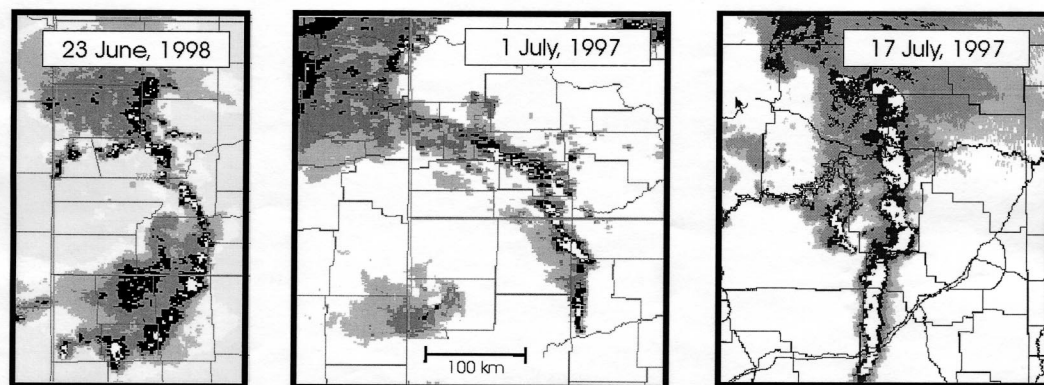

Fig. 8. Examples of severe squall lines observed over the NHP. Radar reflectivity is shaded every 10 dBZ, starting at 20 dBZ.

TABLE 2. Comparison of NHP and Oklahoma (OK) squall lines using the squall-line evolution types of Bluestein and Jain (1985). svr = severe squall lines; non = nonsevere.

Evolution type	Percentage of squall lines of each evolution type					
	OK svr (%)	NHP svr (%)	OK non (%)	NHP non (%)	OK all (%)	NHP all (%)
Broken line	35	44	36	54	35	47
Broken areal	20	47	49	32	35	42
Back building	33	9	13	11	22	10
Embedded areal	12	0	2	3	7	1

with embedded bow echoes (e.g., the 17 July 1997 case in Fig. 8).

Most of the squall lines completed their life cycle within the boundaries of the NHP (cf. Figs. 1 and 7). A typical NHP squall line observed in this study was relatively short lived—averaging just over 3 h from initiation to dissipation (or evolution into another morphology). It is interesting to note that severe-wind-producing squall lines lasted almost 50% longer than their nonsevere counterparts (3.8 versus 2.6 h, respectively). A number of weak and very short-lived (1–1.5 h) squall lines were observed over the NHP. These squall lines were typically initiated along weak troughs or old convective outflows, and were rarely associated with severe weather. The brevity of these storms also compromised their ability to produce areas of stratiform precipitation, which are commonly observed with mature MCSs (Houze et al. 1989).

Despite the relatively short duration of the NHP squall lines in general, stratiform areas of rain were observed within 44% (41) of the squall lines. Using the definitions of Parker and Johnson (2000) for trailing stratiform (TS), parallel stratiform (PS), and leading stratiform (LS) areas of precipitation, it was found that 19 of these events (20% of the total number of NHP squall lines) exhibited TS structure, 19 events PS structure, and 4 events LS structure. These numbers contrast to those in the study of linear MCSs over the Great Plains in Parker and Johnson (2000), who found nearly equal numbers of PS and LS events (each accounting for 19% of the total), but a much greater percentage of TS events (58% of the linear MCSs with stratiform areas were TS events). However, similar to this previous research, it was found that the TS events lived the longest over the NHP, with an average duration of 4.8 h, compared to 3.8 h for PS events, and 2.5 h for LS events. The TS events were also associated with the greatest number of severe wind reports—15 of the 19 TS events had severe winds reported with them, while less than half of either the PS or LS events were associated with severe winds. In general, it was observed that the stratiform regions associated with these squall lines were rather limited in size—perhaps a result of the rather short life span of the NHP squall lines, and the relative lack of lower-tropospheric moisture (as compared with the CP-MIS in section 3b; Fig. 6d).

In order to compare the early evolution of the squall lines observed over the NHP with those of a climatologically different area, the squall lines were analyzed in the same manner as Bluestein and Jain (1985) and Bluestein et al. (1987), who examined severe and nonsevere squall lines over Oklahoma in the spring. As such, the evolutions of the observed squall lines were divided into four types:[4] (i) broken line, (ii) broken areal, (iii) back building, and (iv) embedded areal. The results of these analyses, as well as those of Bluestein and Jain (1985) and Bluestein et al. (1987), are shown in Table 2. Considering both severe and nonsevere squall lines, broken-line and broken-areal evolutions accounted for the majority of the observed evolutions over both regions (70% over Oklahoma, and 89% over the NHP). Back-building squall lines were much less frequently observed over the NHP, with only 10% of the NHP squall lines observed to evolve in this manner (as opposed to 22% over Oklahoma). Embedded-areal-type evolutions were very rare over the NHP from 1996 to 1999, with only one case (1%) exhibiting this behavior, as opposed to 7% of all Oklahoma squall lines. Considering severe squall lines only, the NHP demonstrated a large proportion of broken-areal squall lines, and few back-building lines. Bluestein and Jain (1985) observed that the back-building squall lines developed within environments that favor supercell development (i.e., moderate-to-large CAPE and vertical wind shear). Figure 6 demonstrates that over the CP-MIS area in the spring, the SBCAPE (Fig. 6a), 0–3-km total shear (Fig. 6b), and low-level hodograph curvature (as implied from Fig. 6g) are larger than those parameters over the NHP during the summer, which provide a more favorable environment for supercells. It should also be noted that the nocturnal boundary layer wind maximum (nocturnal low level jet) has been shown to be very important in the development of back-building MCSs (Corfidi 1998), and may also contribute to the greater percentage of

---

[4] The definitions of the four evolutionary types herein are identical to those found in Bluestein and Jain (1985). As a reference, *broken-line* formation involves the nearly coincident appearance of discrete cells, which fill in to form the squall line. *Broken-areal* formation refers to lines that are formed from an amorphous area of moderate to intense cells. *Back-building* lines are dominated by the development of the line upstream (relative to cell motion). *Embedded-areal* formation refers to lines that develop from a previously existing area of weaker, stratiform precipitation.
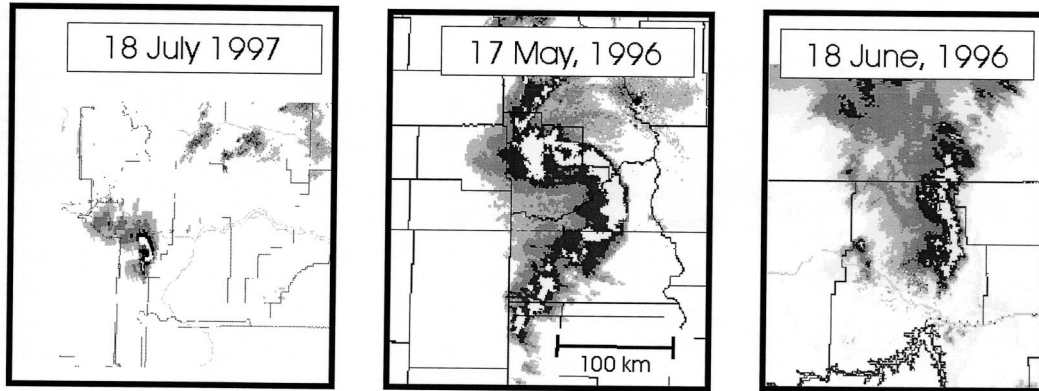
FIG. 9. Same as in Fig. 8 but for severe bow echoes.

back-building squall lines over the southern Great Plains.[5]

c. Bow echoes

Sixty-five bow echoes were observed over the NHP from 1996 through 1999, 56 of which (86%) were associated with severe winds at the surface. These 56 severe bow echoes accounted for 35% of the organized high wind events over the area, and at least 29% of the total number of severe winds reported (note that there were many more squall lines observed, but a smaller percentage of them were associated with severe winds). The NHP bow echoes had a mean lifetime of 3.2 h, over which there was an average of 4.3 severe wind reports. Though severe winds were associated with a majority of the bow echoes (86%), severe hail occurred only in about half of the cases (55%), with wind reports being almost three times as frequent as hail reports. This supports the large body of research that has found that the bow echo convective structure is primarily associated with strong or severe winds (e.g., Przybylinski 1995; Weisman 2001).

Bow echoes observed over the NHP occurred on a variety of scales, from less than 20 km in length for cell–bow echo structures (Lee et al. 1992), to over 120 km for the largest bow echoes. Four of the observed bow echoes were a part of linear MCSs (squall lines); the remaining 60 were mostly isolated from other convection. Typical examples of severe bow echoes observed over the NHP are shown in Fig. 9.

Because the radar appearance of a bow echo can be an *indicator* of severe winds (not a *predictor*), an effort was made to document the early evolution of bow echoes in order to observe any signals that might lead to the production of the downbursts responsible for the

bowing storms. Radar data from early in the evolution of the 65 bow echoes were analyzed, and it was found that the greatest percentage of bow echoes (46%) evolved from "unorganized" groups, or isolated (non-supercellular) storms—that is, clusters of cells or isolated storms without any apparent convective-scale organization. Less frequently, bow echoes formed directly from squall lines (30%) and supercells (24%).

Interestingly, it was found that the initiation of a large percentage (41%) of bow echoes was associated with cell or storm mergers. A typical example of this evolution (which often leads to rapid bow echo development) is shown in Fig. 10. This type of bow initiation was frequently characterized by the existence of a strong (possibly severe) thunderstorm moving with a greater speed than others. In most cases, these "aggressive" storms were moving faster than the 0–6-km mean wind; the disparate motion of which led to an eventual collision or merger. The merging of the cells was typically associated with an increase in the breadth and magnitude of the radar reflectivity, and the production of an arc of reflectivity (bow) within 10–20 min. It is hypothesized that the disruption of storm-scale processes as a result of the merger locally increases the precipitation rate (and associated outflow), thus promoting the formation of cells along the enhanced outflow as it spreads out.
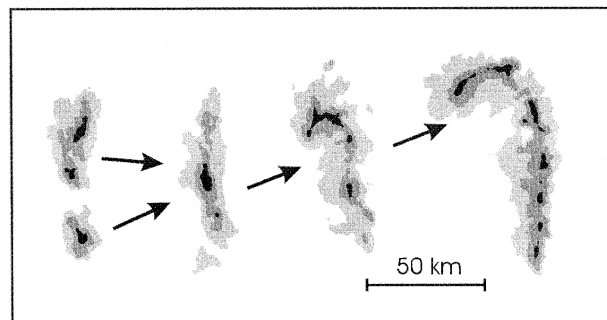

FIG. 10. The 11 June 1998 bow echo case. Radar reflectivity depicts the storm merger and development of the bow echo.

---

[5] An assumption is made that there exists a preference for the nocturnal low-level jet to occur over the southern Great Plains, as suggested by Bonner (1968), Thompson et al. (1976), and Mitchell et al. (1995).
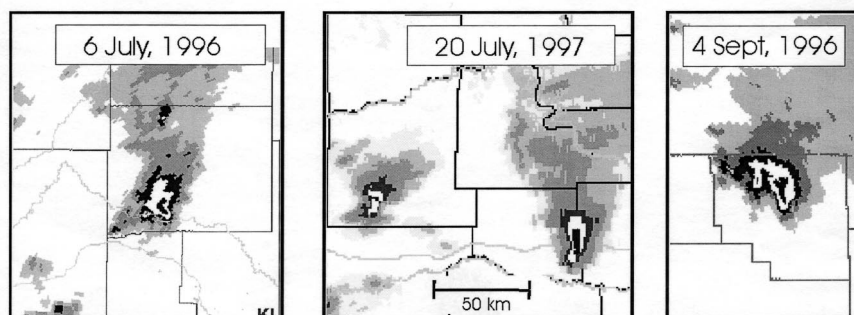
FIG. 11. Same as in Fig. 8 but for high-wind-producing supercells.

The governing processes of the merger–bow echo formation exhibited in the NHP storms could be similar to that demonstrated in the numerical simulations of Finley et al. (2001), who investigated the evolution of a supercell into a bow echo through a merging process. Within squall lines, bow echoes were typically initiated when and where the squall line moved along some pre-existing boundary, or merged with slower-moving cells ahead of the line. While it is outside the scope of this article to address the merger–bow process in detail, the significant number of storms that exhibited this behavior suggests that it is a subject that demands further attention. Squall lines that evolved into a bow echo without any apparent external influence (surface boundary, storm merger, etc.) were relatively rare (<30% of the squall line to bow echo evolution cases).

d. Supercells

Twenty-eight high-wind-producing supercells accounted for 18% of the high wind events over the NHP, and produced 9% of the total number of observed severe wind reports (Table 1). These supercells averaged 2.8 severe wind reports per event, at an average rate of 0.7 per hour. This rate is lower than that of the observed squall lines and bow echoes, but is likely biased downward by the limited spatial extent of supercell thunderstorms. These supercells exhibited the longest life span of all the organized high wind events—lasting an average of 3.9 h. In contrast to the bow echoes and squall lines observed over the NHP, severe hail reports were twice as common as severe winds in the observed high-wind-producing supercell storms. This is not surprising given the more efficient hail production of supercells (Browning 1977). Though the area affected by the supercells was considerably smaller than the other morphologies, these storms were among the most destructive because of the combination of high winds and large hail (e.g., Klimowski et al. 1998).

Most of the high-wind-producing supercells in this study were categorized as high precipitation (HP) in character (e.g., Moller et al. 1994). It was noted that nine (29%) of the supercells evolved into bow echoes

before dissipation, with evolutions similar to that observed in Moller et al. (1994). The supercells examined herein remained discrete, making their identification relatively simple. Several examples of severe-wind-producing supercells observed over the NHP are shown in Fig. 11.

The tracks of the severe-wind-producing supercells observed from 1996 through 1999 are shown in Fig. 7c. The most striking aspect of this figure is the predominance of supercells in a relatively narrow corridor from southeastern Montana through northwestern South Dakota. Over 25% of the observed high-wind-producing supercells moved east or southeast through this area. While it is possible this could be attributed to observational bias (the principal investigators of this research are from western South Dakota), or small sample size, it is remarkable that there is such a frequency of supercells in this particular area north of the Black Hills, rather than to the south, for instance.

The supercells that moved southeast through the Montana–South Dakota corridor were analyzed with respect to ambient synoptic-scale conditions. Surface analyses (not shown) indicate that most of these supercells developed within a postfrontal (or posttrough) surface environment, similar to the pattern observed in Doswell (1980). Significant synoptic-scale forcing was present in most of these cases from upstream shortwave troughs that moved through the area after the passage of the surface front or trough. Perhaps more important is the fact that the surface winds had a significant northerly component in most of these cases. Given the topography of southeastern Montana, which slopes toward higher elevations to the south (not shown), this posttrough wind regime would be directed upslope, and perhaps provided the mechanism needed to initiate convection in this specific area. This synoptic regime also engendered relatively stronger vertical wind shear than in the prefrontal or pretrough environment.

e. Irregular convective systems

Twelve severe-wind-producing irregular groups of storms were documented over the NHP through the anal-
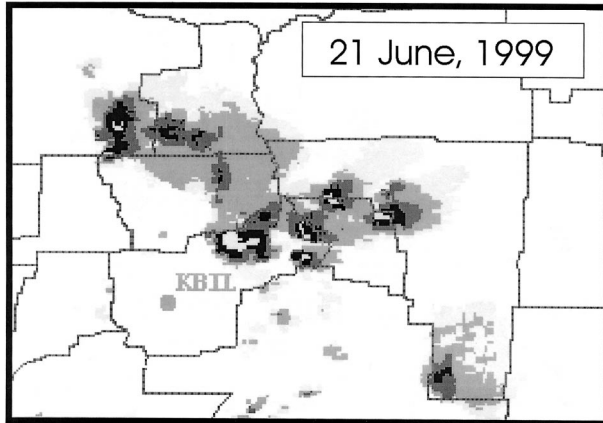
FIG. 12. Same as in Fig. 8 but for a high-wind-producing
irregular group.

ysis period. Essentially, these storms did not fit into any of the other categories (squall line, bow echo, or supercell), but still produced a number of high wind reports in a deliberate pattern. These events accounted for 11% of the organized severe wind events observed, and greater than 7% of the total number of observed high wind reports. Interestingly, the ratio of severe wind to severe hail in these storms was the highest of all the observed high wind morphologies (5:1). Since there was no clearly defined morphology for these storms, the duration or track of these events could not be determined. In general, these events were characterized by the presence of an area of scattered strong to severe storms, moving with roughly the same velocity as the mean tropospheric wind (e.g., Fig. 12). This mode of convective organization was most similar to the broken-areal squall-line evolution, with the exception that a distinct line never actually developed.

5. Environmental analyses

As was described in section 2e, radiosonde data representing the preconvective environments of the observed high wind events and nonsevere squall lines and bow echoes were collected, resulting in 104 (of a possible 198) cases. Sounding data from an additional 102 NHP supercells (independent of any associated severe weather) were also included in these analyses to facilitate a comparison between the high-wind-producing supercells observed from 1996 through 1999 and a larger, all-encompassing supercell dataset over the NHP. Only a small fraction of these soundings were from 1200 UTC (5%), which is consistent with the small percentage of high wind events observed in the early morning (see Fig. 5). Average moisture, instability, and shear parameters from these sounding analyses are shown in Tables 3 and 4 (median values were also calculated, and exhibited qualitatively similar results).

It is apparent in Tables 3 and 4 that the parameters

that best differentiate between the various storm types are those related to moisture and instability, and that the environments associated with the bow echoes represented, in most cases, the greatest parameter values exhibited by the various storm morphologies. For example, average sounding parameters associated with the bow echo environments exhibited the largest SBCAPE (3132 J kg^{-1}), the second smallest SBCIN (-39 J kg^{-1}), the largest low-level mixing ratio (12.6 g kg^{-1}), the largest precipitable water (3.02 cm), and the largest theta-E difference[6] (22.4°C). This SBCAPE is greater than the 95th percentile for all months except June in the NHP [conditional on the SBCAPE (SBCIN) being greater (less) than 50 J kg^{-1}]. Even though most of these average sounding parameter values for bow echoes are larger than those for the other convective modes, the standard deviations show that there is considerable overlap between the sounding parameters, thus limiting their individual usefulness in the forecast setting. The above results are consistent with previous studies of warm-season bow echoes, which indicated that they are frequently associated with extreme buoyancy (Johns and Hirt 1987; Weisman 1992, 1993; Johns 1993; Przybylinski 1995; Evans and Doswell 2001).

In general, the high-wind-producing supercell environments had the second largest mean SBCAPE (2462 J kg^{-1}), the least amount of SBCIN (-38 J kg^{-1}), the lowest SBLCL heights (1256 m), and the second largest theta-E difference (20.8°C). The theta-E differences for both the bow echoes and high-wind-producing supercells agree well with the results of Atkins and Wakimoto (1991), who found values greater than 20°C were supportive of strong downbursts. In summary, the severe bow echoes and high-wind-producing supercells had the largest SBCAPE, the smallest SBCIN, and the largest theta-E differences between the boundary layer and midlevels.

Consistent with the above-mentioned results, the average SBCAPE values decreased for the remainder of the categories from the events more frequently producing severe winds to those producing the least: (i) severe squall lines (1674 J kg^{-1}), (ii) severe irregular groups (1294 J kg^{-1}), and (iii) nonsevere squall lines (1041 J kg^{-1}). Similar trends were noted in the theta-E difference. These results are qualitatively similar to Bluestein and Jain (1985) and Bluestein et al. (1987), who found their CAPE values were higher for the severe squall lines when compared with the nonsevere squall lines across Oklahoma. The differences between the environments of the severe and nonsevere squall lines, with

---

[6] The theta-E difference is defined here as the difference between the largest equivalent potential temperature in the lowest 300 hPa of the sounding (excluding the surface) and the smallest equivalent potential temperature in the entire thermodynamic profile. This is similar to the definition of $\Delta\theta_e$ in the wet microburst study of Atkins and Wakimoto (1991), except that surface data are not used because of potential data quality problems.

TABLE 3. Average values and standard deviations (in parentheses) of thermodynamic parameters derived from the analysis of radiosonde data over the NHP for several severe-wind producing convective storm types. Units: SBCAPE and SBCIN, J kg^{-1}; SBLCL, m; mixing ratio (MXR), g kg^{-1}; precipitable water (PWAT), cm; relative humidity (RH), %; and theta-E difference (TEdiff), K.

Category	Thermodynamic parameter								
	SBCAPE	SBCIN	SBLCL	SBBRN	MXR (surface–1 km)	PWAT (surface–300 hPa)	RH (surface–300 hPa)	TEdiff	No.
Severe wind supercells	2462 (1776)	−38 (60)	1256 (425)	44 (35)	11.2 (2.1)	2.67 (.18)	53 (9)	20.8 (6.6)	19
NHP supercells	2242 (1552)	−58 (98)	1447 (697)	49 (55)	10.2 (2.6)	2.44 (0.20)	50 (11)	18.1 (7.9)	102
Severe wind bow echoes	3132 (2149)	−39 (82)	1280 (547)	79 (67)	12.6 (2.8)	3.02 (0.22)	57 (10)	22.4 (9.2)	22
Severe wind squall lines	1674 (1134)	−57 (85)	1410 (728)	50 (69)	10.4 (2.1)	2.67 (0.20)	54 (13)	17.4 (7.7)	29
Nonsevere squall lines	1041 (804)	−114 (132)	1473 (847)	69 (88)	9.3 (2.4)	2.54 (0.25)	52 (13)	13.4 (6.5)	19
Severe wind irregular groups	1294 (1268)	−122 (110)	1631 (531)	58 (90)	9.9 (2.8)	2.82 (.25)	51 (8)	16.4 (7.9)	9
Avg	1974	−71	1416	58	10.6	2.69	53	18.0	

respect to SBCAPE, SBCIN, and theta-E difference, suggest that there is potential forecasting applicability when using all of these parameters in combination.

There is much less of a difference among the shear-related variables for the NHP convective windstorms, but some items are worth noting (Table 4). First, both supercell categories exhibited the strongest shear overall, and especially in the 0–6-km layer. This supports the notion that supercells occur only when the deep-layer shear reaches a sufficient magnitude (e.g., Chisolm and Renick 1972; Marwitz 1972; Bunkers 2002). Conversely, the nonsevere squall lines displayed the weakest vertical wind shear among all of the categories. Also of interest, the high-wind-producing supercells had nearly the same amount of shear in the 0–3-km layer as was present in the 3–6-km layer; this is a reflection of stronger midtropospheric winds. In summary, the 0–3-km shear was similar among all high-wind-producing categories, and weakest for the nonsevere squall lines, but the relative importance of the low-level shear versus the buoyancy is difficult to ascertain.

In order to better understand the distribution of vertical wind shear, composite hodographs were developed for the severe squall lines, nonsevere squall lines, severe bow echoes, and high-wind-producing supercells. This was accomplished by (i) translating the origin of the hodograph to the point defined by the 0–0.5-km mean wind, (ii) rotating the hodograph such that the 0–6-km wind shear was positive and parallel to the abscissa (to preserve the shape of the hodograph), (iii) averaging the components of the wind as a function of height, and (iv) averaging the components of the storm motion. This technique is a modification of that presented in Rasmussen and Straka (1998).

The composite hodographs support the results of Table 4. First, there is very little difference between the composite hodograph of the severe squall lines (Fig. 13a) and that of the severe bow echoes (Fig. 13c). These two composite hodographs are also very similar to that of the severe irregular groups (not shown). By way of contrast, there is a noteworthy difference between the composite hodographs of the severe and nonsevere squall lines, primarily in terms of an overall weaker flow regime for the nonsevere squall lines (Fig. 13b), which can lead to weaker storm-relative flow in the midlevels. Combined with the relatively higher SBLCLs for the nonsevere squall lines, this may act to allow the gust front to outrun the storm, resulting in a premature demise to the system. Also of interest, the hodograph structure for all categories is generally unidirectional, even for the high-wind-producing supercells (Fig. 13d). This is in contrast to the composite hodograph for the 102 NHP supercells (not shown), where clockwise hodograph curvature is more pronounced. In support of this, Johns and Hart (1993) found that unidirectional hodographs were more likely to be associated with outbreaks of damaging winds, whereas strong clockwise curvature was prevalent in tornado outbreak cases.

TABLE 4. Average values and standard deviations (in parentheses) of shear parameters (m s^{-1}) derived from the analyses of radiosonde data over the NHP for several convective storm types. See the appendix for a description of the shear calculations.

	Shear parameter			
	0–3-km total	0–3-km bulk	0–6-km total	0–6-km bulk
Severe wind supercells	20.1 (5.8)	15.9 (5.6)	36.2 (8.7)	27.4 (7.8)
NHP supercells	22.1 (6.7)	16.8 (5.6)	37.1 (6.9)	25.6 (8.9)
Severe wind bow echoes	21.0 (8.4)	15.3 (5.1)	34.0 (10.8)	22.4 (7.3)
Severe wind squall lines	21.8 (6.8)	15.5 (5.8)	35.4 (10.0)	20.7 (5.3)
Nonsevere squall lines	20.4 (5.5)	13.6 (5.9)	33.7 (8.0)	17.1 (5.8)
Severe wind irregular	20.7 (8.6)	15.1 (7.1)	34.9 (9.9)	21.3 (9.2)
Avg	21.0	15.4	35.2	22.4

The stronger overall shear of the high-wind-producing supercells, combined with the larger theta-E differences (relative to the 102 NHP supercells), are consistent with the results of Gilmore and Wicker (1998). In general, they found that when the vertical wind shear is relatively large, in the presence of midtropospheric dryness (as implied by the large theta-E difference), the low-level outflow does not dominate the supercell and, therefore, is not as detrimental to the storm longevity. This suggests that the supercell could persist for a longer period of time given the conditions in Fig. 13d, allowing for a greater chance of severe weather to be observed.

6. Conclusions

In this research, we set out to determine what convective storm types were responsible for the production of severe winds over the NHP, identify the general environmental characteristics associated with the identified storm types, and compare our results with those of
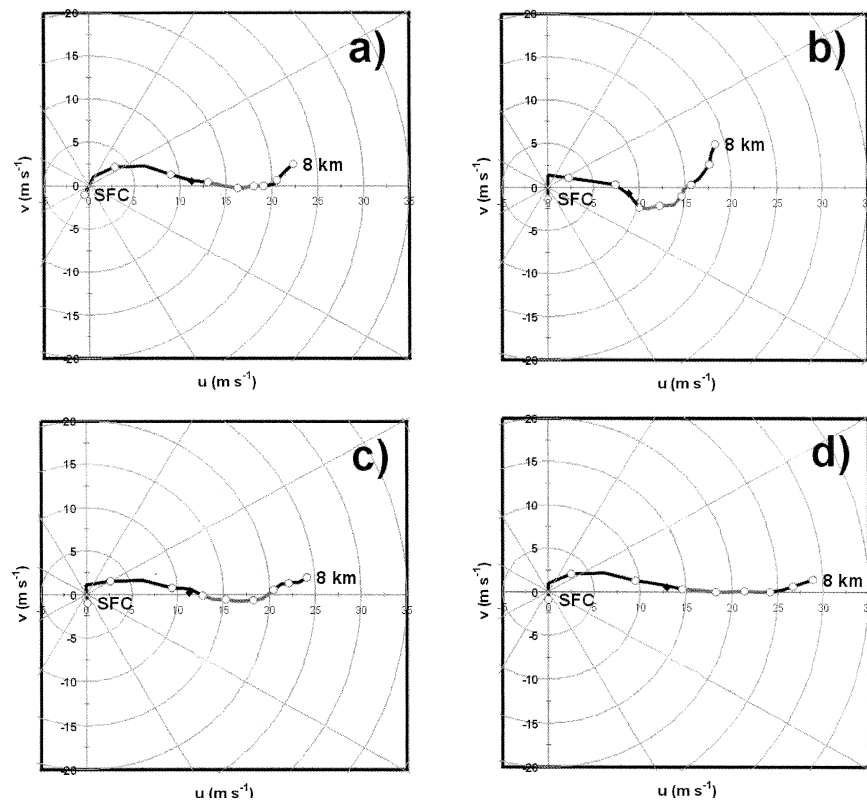

FIG. 13. Composite hodographs derived from radiosonde data within the environments of the primary severe-wind-producing storm types over the NHP: (a) severe-wind-producing squall lines, (b) nonsevere squall lines, (c) severe-wind-producing bow echoes, and (d) severe-wind-producing supercells. Circles on the hodographs are plotted every 1 km AGL. Black diamonds represent the mean 0–6-km wind for each hodograph.

similar investigations. The main conclusions of this study are as follows:

- Analyses of the severe wind occurrence over the NHP as a function of storm structure indicated that the majority of the observed severe winds were the result of bow echoes (29%) or squall lines (20%), with a smaller percentages from supercells and irregular groups (9% and 7%, respectively).
- Across the NHP, severe winds were reported at a frequency 3 times that of severe hail in bow echoes, and 1.5 times that of severe hail in squall lines. In high-wind-producing supercells, severe winds occurred with about one-half the frequency of severe hail.
- The average life span of NHP convective severe wind events was ~2–4 h.
- Convective mergers were associated with the production of 41% of the observed bow echoes.
- The environmental SBCAPE was largest for the severe bow echoes, which produced the greatest frequency of severe wind reports across the NHP.
- The boundary layer to midtropospheric theta-E difference was largest in the environments of severe bow echoes and high-wind-producing supercells.
- The 0–3-km total shear was quite similar for all severe wind categories. The 0–3-km bulk shear was noticeably lower in the environments of nonsevere squall lines.
- The hodograph curvature in severe-wind-producing supercell environments was less then the hodograph curvature in tornadic supercell environments.

This research elucidates the origin, nature, and environments of severe convective winds across the northern High Plains—critical pieces of information utilized in short-term weather forecasting and the warning process. This research also serves as a first step in understanding the regional differences in severe-wind-producing convective storms, which can be used to our advantage in accurately forecasting convective weather.

APPENDIX

Sounding Data Quality Control and Analysis

Although the sounding data have been extensively quality controlled by NCDC and FSL, including a hydrostatic check, there are several potential radiosonde data quality problems that could still arise in the present dataset (e.g., see Schwartz 1990; Elliott and Gaffen 1991; Schwartz and Doswell 1991; Elliott et al. 2002). Some of the more noticeable errors can result from erroneous data transmission and manual surface data entry. Therefore, additional checks were performed as follows: (i) check for missing data of any kind, and delete that level if data were missing—except for dewpoint as noted below, (ii) check if the surface wind speed was greater than 25 m s^{-1}, and omit sounding if this was the case, (iii) check if the meteorological variables were within reasonable constraints (e.g., the wind direction was between 0° and 360°), and delete that level if data were out of tolerance, (iv) check for "extreme" temperature and dewpoint lapse rates, and delete that level if extreme lapse rates were found, (v) check that the sounding reached 110 hPa, and omit sounding if this level was not attained, and (vi) if the dewpoint was missing, it was set equal to the temperature minus 30°C. At least five levels were required for a sounding to be accepted, which included the surface level. In general, 10% of the soundings were rejected based on this quality-control procedure, with much of the bad data resulting from erroneous surface temperatures.

The virtual temperature correction as described in Doswell and Rasmussen (1994) was performed by 1) determining the parcel ascent path using the observed, and unmodified, sounding data, 2) applying the virtual temperature correction to both the sounding temperature (using the sounding mixing ratio) and the parcel ascent path (using the mixing ratio along the parcel ascent path), and 3) calculating the CAPE using the virtually corrected data. This correction is employed to take into account density (and hence buoyancy) differences due to atmospheric water vapor. The lifting condensation level (LCL) is the same for both the corrected and uncorrected data; however, the CAPE, convective inhibition (CIN), level of free convection (LFC), and equilibrium level (EL) are different for corrected versus uncorrected data (for a more thorough discussion of this topic, see the information available online at http://www.cimms.ou.edu/~doswell/virtual/virtual.html). The equations for potential temperature, equivalent potential temperature, and saturation vapor pressure as defined in Bolton (1980) were also used.

The wind shear was calculated using two different techniques. First, the bulk wind shear was determined by taking the vector difference between the surface and 500-m mean wind and the wind at a higher level (e.g., 3 km). Second, the total (also called cumulative) wind shear was obtained by summing the vertical wind shear

throughout the depth of the hodograph at 0.5-km intervals, up to the desired level (e.g., 3 km). The total shear is a measure of hodograph length and is analogous to ''stretching out'' the hodograph and calculating the bulk shear. For a purely unidirectional hodograph that does not fold back on itself, the bulk shear and total shear must be equal; for a curved hodograph, the bulk shear will always be less than the total shear, oftentimes by a factor of 2 (as seen in the present dataset). It is important to note that the magnitudes of deep-layer shear are dependent upon the vertical sampling interval, which is 0.5 km in the present study.

REFERENCES

Atkins, N. T., and R. M. Wakimoto, 1991: Wet microburst activity over the southeastern United States: Implications for forecasting. *Wea. Forecasting,* **6,** 470–482.

Bentley, M. L., and T. L. Mote, 1998: A climatology of derecho-producing mesoscale convective systems in the central and eastern United States. Part I: Temporal and spatial distribution. *Bull. Amer. Meteor. Soc.,* **79,** 2527–2540.

Bluestein, H. B., and M. H. Jain, 1985: Formation of mesoscale lines of precipitation: Severe squall lines in Oklahoma during the spring. *J. Atmos. Sci.,* **42,** 1711–1732.

——, G. T. Marx, and M. H. Jain, 1987: Formation of mesoscale lines of precipitation: Nonsevere squall lines in Oklahoma during the spring. *Mon. Wea. Rev.,* **115,** 2719–2727.

Bolton, D., 1980: The computation of equivalent potential temperature. *Mon. Wea. Rev.,* **108,** 1046–1053.

Bonner, W. D., S. Esbensen, and R. Greenberg, 1968: Kinematics of the low-level jet. *J. Appl. Meteor.,* **7,** 339–347.

Browning, K. A., 1977: The structure and mechanism of hailstorms. *Hail: A Review of Hail Science and Hail Suppresion, Meteor. Monogr.,* No. 38, Amer. Meteor. Soc., 1–43.

Bunkers, M. J., 2002: Vertical wind shear associated with left-moving supercells. *Wea. Forecasting,* **17,** 845–855.

Changnon, S. A., 2001: Thunderstorm rainfall in the conterminous United States. *Bull. Amer. Meteor. Soc.,* **82,** 1925–1940.

Chisolm, A. J., and J. H. Renick, 1972: The kinematics of multicell and supercell Alberta hailstorms. Alberta Hail Studies, Research Council of Alberta Hail Studies Rep. 72-2, 24–31.

Corfidi, S. F., 1998: Forecasting MCS mode and motion. Preprints, *19th Conf. on Severe Local Storms,* Minneapolis, MN, Amer. Meteor. Soc., 626–629.

Court, A., and J. F. Griffiths, 1986: Thunderstorm climatology. *Thunderstorm Morphology and Dynamics,* E. Kessler, Ed., University of Oklahoma Press, 9–39.

Doswell, C. A., III, 1980: Synoptic scale environments associated with high plains severe thunderstorms. *Bull. Amer. Meteor. Soc.,* **61,** 1388–1400.

——, and E. N. Rasmussen, 1994: The effect of neglecting the virtual temperature correction on CAPE calculations. *Wea. Forecasting,* **9,** 625–629.

——, and L. F. Bosart, 2002: Extratropical synoptic-scale processes and severe convection. *Severe Convective Storms, Meteor. Monogr.,* No. 50, Amer. Meteor. Soc., 27–69.

Easterling, D. R., and P. J. Robinson, 1985: The diurnal variation of thunderstorm activity in the United States. *J. Climate Appl. Meteor.,* **24,** 1048–1058.

Elliott, W. P., and D. J. Gaffen, 1991: On the utility of radiosonde humidity archives for climate studies. *Bull. Amer. Meteor. Soc.,* **72,** 1507–1520.

——, R. J. Ross, and W. H. Blackmore, 2002: Recent changes in NWS upper-air observations with emphasis on changes from VIS to Vaisala radiosondes. *Bull. Amer. Meteor. Soc.,* **83,** 1003–1017.

Evans, J. S., and C. A. Doswell III, 2001: Examination of derecho

environments using proximity soundings. *Wea. Forecasting,* **16,** 329–342.

Finley, C. A., W. R. Cotton, and R. A. Pielke Sr., 2001: Numerical simulation of tornadogenesis in a high-precipitation supercell. Part I: Storm evolution and transition into a bow echo. *J. Atmos. Sci.,* **38,** 1597–1629.

Fujita, T. T., 1978: Manual of downburst identification for Project Nimrod. Satellite and Mesometeorology Research Paper 156, Dept. of Geophysical Sciences, University of Chicago, 104 pp.

——, 1981: Tornadoes and downbursts in the context of generalized planetary scales. *J. Atmos. Sci.,* **38,** 1511–1534.

Geerts, B., 1998: Mesoscale convective systems in the southeast United States during 1994–95: A survey. *Wea. Forecasting,* **13,** 860–869.

Gilmore, M. S., and L. J. Wicker, 1998: The influence of midtropospheric dryness on supercell morphology and evolution. *Mon. Wea. Rev.,* **126,** 943–958.

Hart, J. A., and P. R. Janish, 1999: SeverePlot: Historical Severe Weather Report Database Version 2.0. Storm Prediction Center, Norman, OK. [Available online at http://www.spc.noaa.gov/software/svrplot2/index.html.]

Houze, R. A., Jr., M. I. Biggerstaff, S. A. Rutledge, and B. F. Smull, 1989: Interpretation of Doppler weather radar displays of midlatitude mesoscale convective systems. *Bull. Amer. Meteor. Soc.,* **70,** 608–619.

Johns, R. H., 1993: Meteorological conditions associated with bow echo development in convective storms. *Wea. Forecasting,* **8,** 294–299.

——, and W. D. Hirt, 1987: Derechoes: Widespread convectively induced windstorms. *Wea. Forecasting,* **2,** 32–49.

——, and J. A. Hart, 1993: Differentiating between types of severe thunderstorm outbreaks: A preliminary investigation. Preprints, *17th Conf. on Severe Local Storms,* St. Louis, MO, Amer. Meteor. Soc., 46–50.

——, and J. S. Evans, 2000: Comments on ''A climatology of derecho-producing mesoscale convective systems in the central and eastern United States, 1986–95. Part I: Temporal and spatial distribution.'' *Bull. Amer. Meteor. Soc.,* **81,** 1049–1054.

Kelly, D. L., J. T. Schaefer, and C. A. Doswell III, 1985: Climatology of nontornadic severe thunderstorm events in the United States. *Mon. Wea. Rev.,* **113,** 1997–2014.

Klimowski, B. A., M. R. Hjelmfelt, M. J. Bunkers, D. Sedlacek, and L. R. Johnson, 1998: Hailstorm damage observed from the *GOES-8* satellite: The 5–6 July 1996 Butte–Meade storm. *Mon. Wea. Rev.,* **126,** 831–834.

——, R. Przyblinski, G. Schmocker, and M. R. Hjelmfelt, 2000: Observations of the formation and early evolution of bow echoes. Preprints, *20th Conf. on Severe Local Storms,* Orlando, FL, Amer. Meteor. Soc., 44–47.

Lee, W.-C., R. M. Wakimoto, and R. E. Carbone, 1992: The evolution and structure of a ''bow-echo–microburst'' event. Part II: The bow echo. *Mon. Wea. Rev.,* **120,** 2211–2225.

Maddox, R. A., 1980: Mesoscale convective complexes. *Bull. Amer. Meteor. Soc.,* **61,** 1374–1387.

Marwitz, J. D., 1972: The structure and motion of severe hailstorms. Part I: Supercell storms. *J. Appl. Meteor.,* **11,** 166–179.

McAnelly, R. L., and W. R. Cotton, 1989: The precipitation life cycle of mesoscale convective complexes over the central United States. *Mon. Wea. Rev.,* **117,** 784–808.

Mitchell, M. J., R. W. Arritt, and K. Labas, 1995: A climatology of the warm season Great Plains low-level jet using wind profiler observations. *Wea. Forecasting,* **10,** 576–591.

Moller, A. R., C. A. Doswell III, M. P. Foster, and G. R. Woodall, 1994: The operational recognition of supercell thunderstorm environments and storm structures. *Wea. Forecasting,* **9,** 327–347.

OFCM, 1980: *Weather Radar Observations Part A.* Federal Meteorological Handbook, No. 7, Office of the Federal Coordinator for Meteorology, 5-1–5-2. [Available OFCM, Suite 1500, 8455 Colesville Rd., Silver Springs, MD 20910.]

Orville, R. E., and G. R. Huffines, 2001: Cloud-to-ground lightning

in the United States: NLDN results in the first decade, 1989–98. *Mon. Wea. Rev.,* **129,** 1179–1193.

Parker, M. D., and R. H. Johnson, 2000: Organizational modes of midlatitude mesoscale convective systems. *Mon. Wea. Rev.,* **128,** 3413–3436.

Przybylinski, R. W., 1995: The bow echo: Observations, numerical simulations, and severe weather detection methods. *Wea. Forecasting,* **10,** 203–218.

Rasmussen, E. N., and J. M. Straka, 1998: Variations in supercell morphology. Part I: Observations of the role of upper-level storm-relative flow. *Mon. Wea. Rev.,* **126,** 2406–2421.

Rotunno, R., J. B. Klemp, and M. L. Weisman, 1988: A theory for strong, long-lived squall lines. *J. Atmos. Sci.,* **45,** 463–485.

Schmidt, J. M., and W. R. Cotton, 1989: A High Plains squall line associated with severe surface winds. *J. Atmos. Sci.,* **46,** 281–302.

Schwartz, B. E., 1990: Regarding the automation of rawinsonde observations. *Wea. Forecasting,* **5,** 167–171.

——, and C. A. Doswell III, 1991: North American radiosonde observations: Problems, concerns, and a call to action. *Bull. Amer. Meteor. Soc.,* **72,** 1885–1896.

Smull, B. F., and R. A. Houze Jr., 1985: A midlatitude squall line with a trailing region of stratiform rain: Radar and satellite observations. *Mon. Wea. Rev.,* **113,** 117–133.

Thompson, O. E., P. A. Arkin, and W. D. Bonner, 1976: Diurnal variations of the summertime wind and force field at three midwestern locations. *Mon. Wea. Rev.,* **104,** 1012–1022.

Wakimoto, R. M., 1985: Forecasting dry microburst activity over the High Plains. *Mon. Wea. Rev.,* **113,** 1131–1143.

——, 2002: Convectively driven high wind events. *Severe Convective Storms, Meteor. Monogr.,* No. 50, Amer. Meteor. Soc., 255–298.

Weisman, M. L., 1992: The role of convectively generated rear-inflow jets in the evolution of long-lived mesoconvective systems. *J. Atmos. Sci.,* **49,** 1826–1847.

——, 1993: The genesis of severe, long-lived bow echoes. *J. Atmos. Sci.,* **50,** 645–670.

——, 2001: Bow echoes: A tribute to T. T. Fujita. *Bull. Amer. Meteor. Soc.,* **82,** 97–116.

Zajac, B. A., and S. A. Rutledge, 2001: Cloud-to-ground lightning activity in the contiguous United States from 1995 to 1999. *Mon. Wea. Rev.,* **129,** 999–1019.